Preparation, surface characterization and dielectric studies of hydrogen irradiated Cu/PANI polymer composites

A. Atta[a], B. M. Alotaibi[b,*], H. A. Al-Yousef[b], A. M. Abdel-Reheem[c]
[a]*Physics Department, College of Science, Jouf University, P.O. Box: 2014, Sakaka, Saudi Arabia*
[b]*Physics Department, College of Science, Princess Nourah bint Abdulrahman University, Riyadh, Saudi Arabia*
[c]*Radiation Physics Department, National Center for Radiation Research and Technology, Egyptian Atomic Energy Authority (EAEA), Egypt*

In this study, a PANI/Cu nanocomposite films are prepare using ion sputtering technique. Then PANI/Cu nanocomposite films are irradiated by different fluence of low energy hydrogen ion ($1x10^{16}$, $4x10^{16}$, and $8x10^{16}$ ion/cm^2). The changes in crystallite structure are studied using XRD diffractometer. The dielectric properties and the energy density of the blank and irradiated films are obtained at room temperature in the frequency range of 100 to 5MHz. The measurements indicated significant changes in these parameters after hydrogen ion irradiation. The dielectric constant ε' improved from 1.5 for PANI/Cu to 6, 10 and 23 after exposed to $1x10^{16}$, $4x10^{16}$, and $8x10^{16}$ ion/cm^2. Moreover, the conductivity energy density is improved from $1.6x10^{-5}$ for unirradiated to $2.1x10^{-5}$, $4.8x10^{-5}$, and $1.5x10^{-4}$ for irradiated films. The results confirmed an improving in electric properties and energy density of the irradiated PANI/Cu nanocomposite films, which can using these films in wide range of application such as super-capacitor and microelectronic devices.

Received January 2, 2023; Accepted April 7, 2023)

Keywords: Surface characterization, Ion beam, Electrical properties, Polymer composites

1. Introduction

Conductive polymers including polyaniline (PANI) has received a good deal of interesting due to their light weight, high electro activity, and high aspect ratio [1]. For these reasons, conductive polymers have many applications in cellular phones, televisions, light-emitting diodes, displays, batteries, solar cells, sensors, and microelectronics [2]. Additionally, conductive polymers and their composites also have a perfect electromagnetic absorption property, which makes them useful for eliminating electromagnetic radiation [3]. PANI has many advantages such as easy fabrication, redox properties, low cost, wide range of conductivity, and environmental friendliness [4]. However, the employment of PANI is bounded due to its pauper solubility, mechanical properties, fusibility, and processability [5]. Polymer nanocomposites with superb dielectric properties are robustly desirable for electronic devices and super-capacitors. Consequently, the electrical and dielectric properties of the polymer can be amended by employing ion beam irradiation due to the important processes which occur inside polymer, e.g., cross-linking, free radical formation, oxidation, carbonization, and macromolecular distribution [6].

The polymer–metal nanocomposites are making these as promising materials for various applications. The characteristics of the metal nanoparticles such as optical, electronic, magnetic, and catalytic are depend on their size, and the shape of the crystal [7, 8]. The sputtering is a suitable method for manufacturing of integrated circuits and microsystems or semiconductors interconnects [9] and multilayer [10,11]. The electrical conductivity of commercially copper is lower costs and accessibility causes, that Cu is the metal used most often in electronic applications [12]. The control of grain size is special importance in deposition of semiconductors, because of

* Corresponding author: bmalotaibi@pnu.edu.sa
https://doi.org/10.15251/DJNB.2023.182.475

the grain size-band gap dependence [13]. The grain size effect on physical properties is also a particularly important in contact surfaces for electronic applications [14].

Consequently, the electrical properties of the polymer can be amended by employing ion beam irradiation. Because ion irradiation of polymer lead to important processes inside polymer such as cross-linking, free radicals formation, oxidation, carbonization, and macromolecular distribution [15,16]. In the present work, we fabricated nanocomposite films of PANI/Cu using an ion beam sputtering technique to sputter Cu nanoparticle into PANI polymer. After that, the films are irradiated by different fluence of hydrogen ion $1x10^{16}$, $4x10^{16}$, and $8x10^{16}$ion/cm^2. The dielectric properties, electric modulus, and the energy density efficiency of the pure and irradiated films are deduced at constant temperature 20^o C in the frequency range of 100 to 5MHz.

2. Experimental work

PANI is dissolved in Dimethylformamide (DMF) for 60 min at room temperature by using ultra sonic probe and then casting the film in Petrie dish for 1 day. Also; the cold cathode ion source sputtering technique as shown in Figure 1 is used to sputter copper nanoparticles into the PANI polymer for 30 mints and mixed using ultra sonic probe. The sputtering technique is a cold cathode ion source which described previously [17] with conditions; sputter time 30 min using Ar gas at energy 4keV and pure copper target (99.97) is placed by angle 60^o on the front beam. The PANI/Cu nanocomposite film is prepared successfully using sputtering technique. This method obtained copper in small range of nano because the sputter steps are started from single atom to more atoms and growth into island from atoms to forming the crystals. The prepared film is cutting into 1cm x 1cm samples to be irradiated and characterized. The ion source is used for irradiated the samples after preparation the samples using hydrogen gas at energy 5keV and ion current 100μA using different fluence $1x10^{16}$, $4x10^{16}$, and $8x10^{16}$ ion/cm^2.

The structural properties for PANI/Cu nanocomposites films are studied using XRD (Shimadzu XRD-6000) with Cu Kα radiation (λ=1.5406Å). A Transmission Electron Microscope (TEM) is used for recording high magnification image of samples. The electric properties, electric modulus properties of the un-irradiated and irradiated films measured in the temperature range from 293-353 K, where a programmable automatic RLC bridge (HIOKI 3532 LCR HITESTER) at frequency from 100 Hz to 5MHz used to measure the impedance Z, the capacitance, and the loss tangent (tan δ) directly

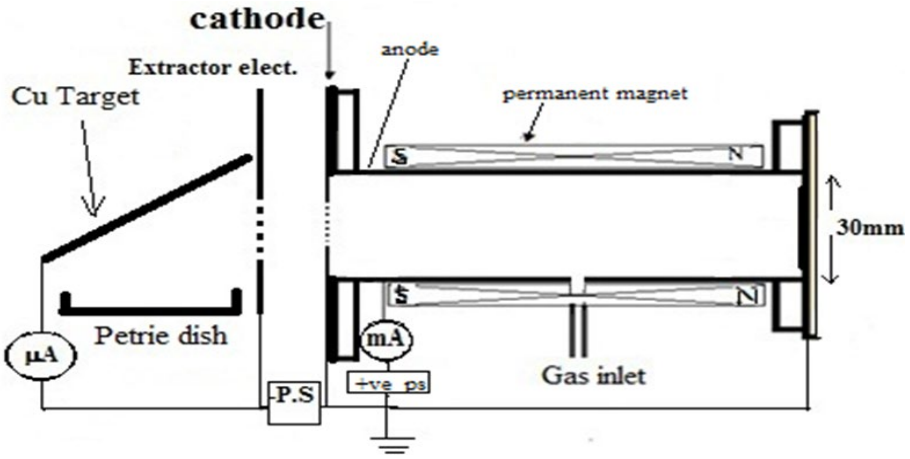

Fig. 1. Sputtering technique low energy ion source.

3. Results and discussion

When an ion collides with the target, penetrated in it depend on the nature of the material's composition. The incoming ions lose their energy in the target in different images such as displacement of target atoms and phonon i.e. the simulation process was executed by using the SRIM/TRIM simulation code [18]. The distribution depth of bombarded ions depends on their energy, fluence, type, and also on the type and structural of target material [19]. Figure 2a shows the average projected range for 5keV hydrogen ion is 107 nm and ion straggling is 33nm. Also, figure 2b shows the collision events; the target vacancies are 7/ion, target displacements (number of atoms knocked off their target lattice site) are 7/ion. The obtained target vacancies are equals the target displacements, i.e. the replacements is zero. Figure 2c shows the energy to recoil; where the energy absorbed by C is larger than the H or N atoms. Figure (2d) shows the energy loss to phonons, where the phonons are the energy stored in atomic vibrations in a crystal of the target. All phonon come equally from ions and recoil atoms. Also; the energy deposited by recoil is 6.34% from incident energy and the energy loss from ions is 90% for ionization, 0.2% for vacancies and 3.42% for phonon.

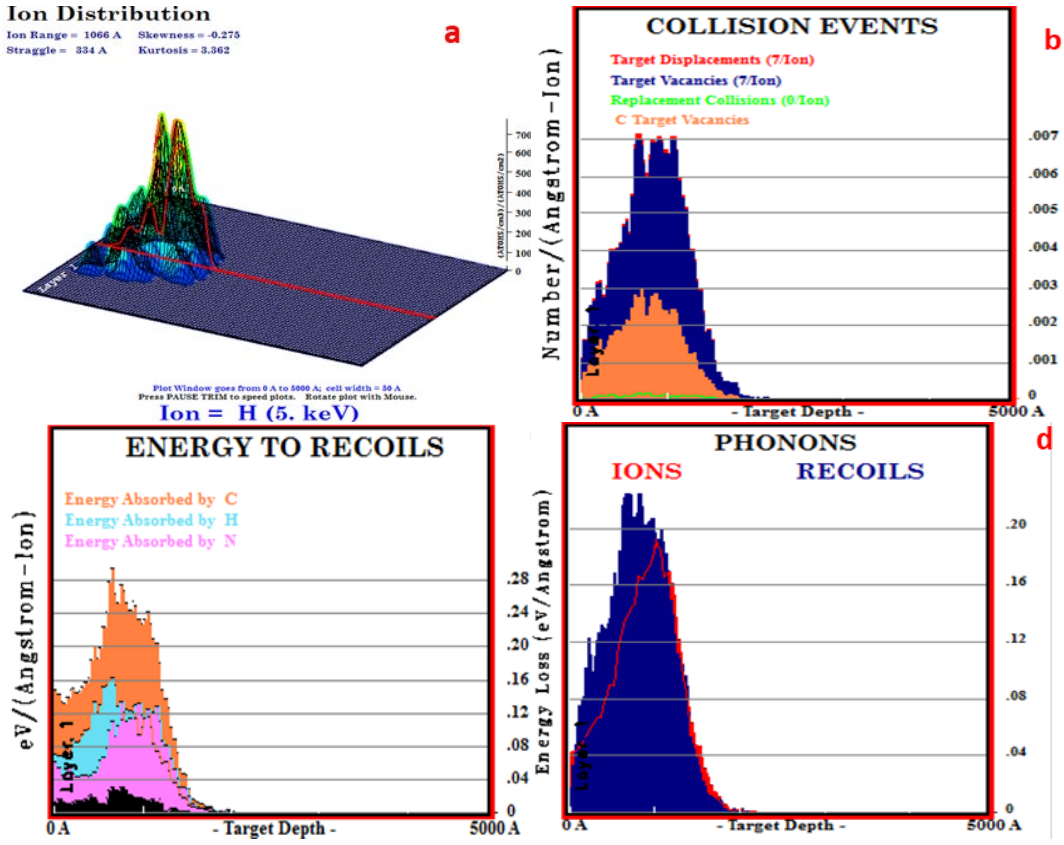

Fig. 2. SRIM/TRIM simulation for hydrogen ions collide with PANI/Cu films.

The X-ray diffraction is one of the most important characterization tools used in materials science. Diffraction pattern gives information on translational symmetry - size and shape of the unit cell from peak positions and information on electron density inside the unit cell, namely where the atoms are located from peak intensities. Figures 3a shows the XRD patterns recorded for PANI/Cu film. The XRD patterns show a preferred three peak for Cu of 2θ at 43.1 ° and 50.3 ° corresponds to 111 and 200 after sputter time of 30 min. Figure 3b shows the XRD spectrum of PANI/Cu film after exposed to hydrogen fluence of $1x10^{16}$, $4x10^{16}$, and $8x10^{16}$ion/cm^2. The changes in crystalline structure after hydrogen ion irradiation is due the interaction of the PANI/Cu

film with the hydrogen beam, which results in the induced rearrangement of PANI/Cu crystal structure after irradiation, causes a modification in XRD peak intensity after irradiation.

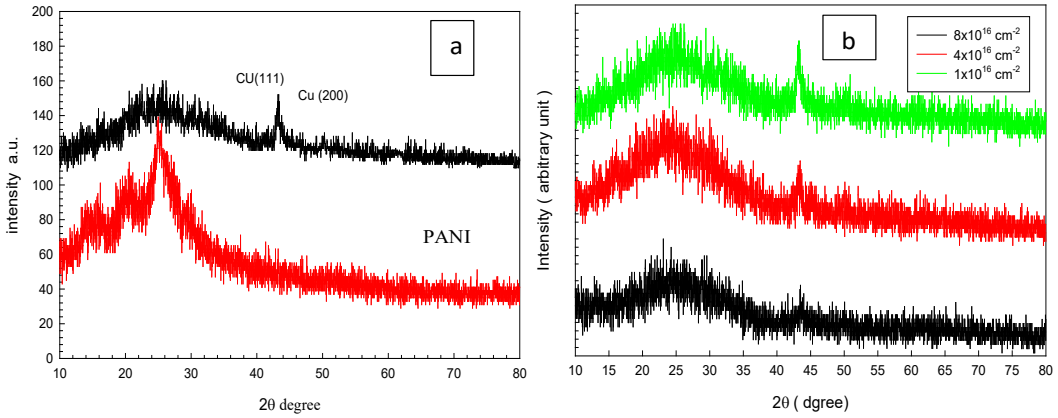

Fig. 3. XRD for (a) Pure PANI and untreated PANI/Cu, (b) irradiated PANI/Cu with different fluence of hydrogen beam.

The average crystallite size is obtained using Debye-Scherrer formula [20]

$$D = \frac{0.9\lambda}{\beta \cos\theta} \tag{1}$$

where 'λ' is wave length 1.541 A^{o} of X-rays used, 'β' is FWHM in radian,' θ' is the diffraction angle in degree and 'D' is crystallite diameter size. The crystallite size of Cu nano is found to be 22 nm before ion irradiation and are 20, 18, and 14nm after hydrogen ion irradiation with fluence 1x10^{16}, 4x10^{16} and 8x10^{16} ion.cm^{-2} respectively. The value of interplanar spacing d is calculated by [20]:

$$\mathrm{d} = \frac{\lambda}{2\sin\theta} \tag{2}$$

The interplanar spacing is 0.21 for blank is changed to 0.205 and 0.2 nm after hydrogen ion irradiation with fluence 4x10^{16} and 8x10^{16} ion.cm^{-2} respectively. A Transmission Electron Microscope (TEM) is used for recording high magnification image of samples as shown in figure 4a,b. Figure 4a show the sample image before ion irradiation and 4b the sample after ion irradiation by fluence 8x10^{16}ion/cm^{2} the particle size is decreased after ion irradiation from 22 to 16 nm.

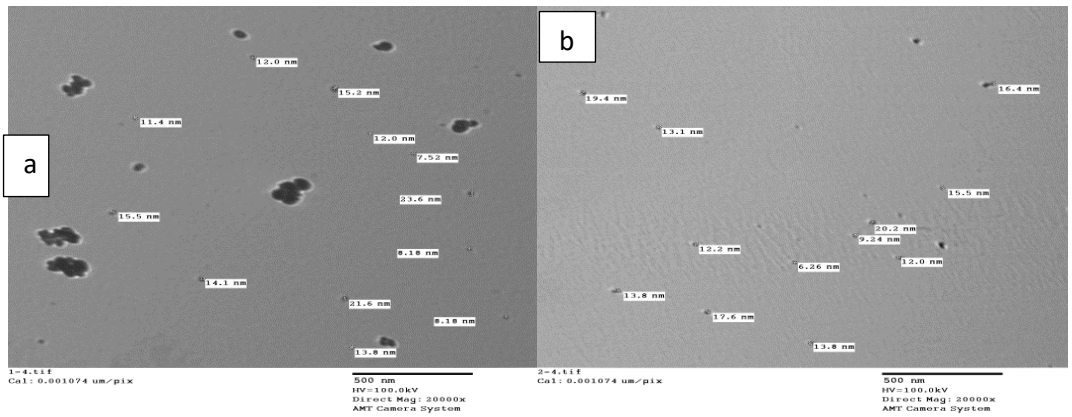

Fig. 4. TEM images of (a) untreated PANI/Cu and (b) irradiated PANI/Cu of 8x10^{16} ion.cm^{-2}.

The complex dielectric permittivity (ε*) given by the relation:

$$\varepsilon^* = \varepsilon' - i\,\varepsilon'' \tag{3}$$

where ε' represents the dielectric constant which demonstrates the capacity of a material to storage electric charge [21]. Therefore, polymer nanocomposites which have high dielectric constant are employed for electronics applications and energy storage. Moreover, the dielectric constant of blank and irradiated films has been calculated by the following expression [22].

$$\varepsilon' = \frac{Ct}{\varepsilon_o A} \tag{4}$$

where; C is the capacitance, t the thickness of films, and A is the area of dielectric. Figure 5 shows the change of ε' with the frequency of applied electric field at constant temperature for the blank and irradiated films. It is observed that ε' of irradiated samples have the same behavior of un-irradiated films. Also; there is a significantly large increases in ε' value after irradiation, which gradually increases with increasing hydrogen ion fluence. As shown in Table 1, the dielectric constant for PANI/Cu at frequency 100 Hz is 1.5 and increases to 6, 10, and 23 when exposed to $1x10^{16}$, $4x10^{16}$, and $8x10^{16}$ ion/cm^2, respectively. This is because of the more defects producing in the band gaps of polymer model as a result of chain scission [23]. In particular, values of ε' increase with increasing the irradiation fluence due to breaking of bonds that increase number of defects in polymer system.

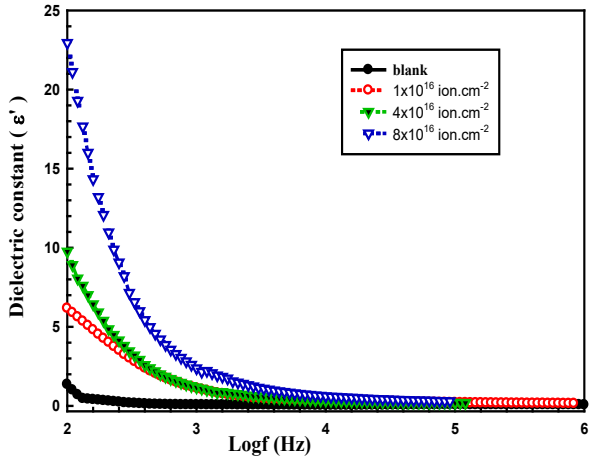

Fig. 5. Frequency dependence of the dielectric constant for PANI/Cu nanocomposites films.

Specially, ε'' refers to the imaginary part of the complex dielectric and called dielectric loss which usually measured by loss tangent tan (δ) values. Where, it demonstrates the proportion among the amount of energy wasted in a material to the amount of energy stoked in a material, and it was calculated through using the next relationship [24,25]:

$$\varepsilon'' = \varepsilon' \tan\delta \tag{5}$$

where δ = (90º-θ) and θ is the phase angle. The variation of dielectric loss as a function of frequency of the pristine and irradiated nanocomposite samples are show in Figure 6. It can be seen that ε" values of the irradiated films is a significantly large increases in ε" after irradiation by different doses of hydrogen ion this due to the defects that creating in the band gaps of polymer as a result of chain scission. Then the values of ε" gradually increase with increasing ion irradiation due to breaking of bonds that increase number of defects in polymer system [26]. In which, ε"

value of the nanocomposite film increase after irradiation, which increases from 16 for PANI/Cu to 58, and 96 after irradiation by $4x10^{16}$ and $8x10^{16}$ ions/cm^2, respectively.

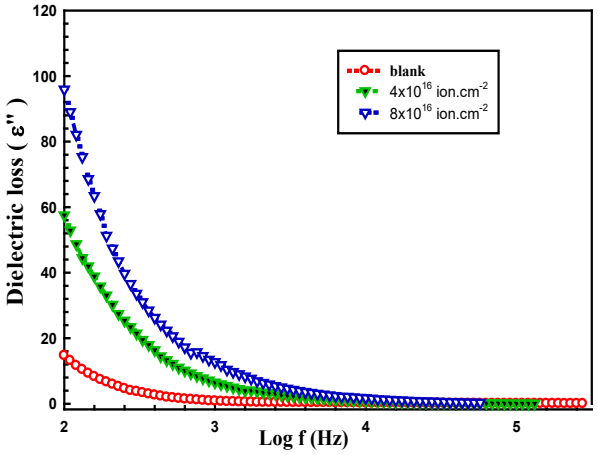

Fig. 6. Dielectric loss of the unirradiated and irradiated PANI/Cu nanocomposites films.

The AC electrical conductivity (σ_{ac}) of most polymers changes with the frequency according to the percolation relation [27,28]:

$$\sigma_{ac} = \varepsilon_o \varepsilon'' \omega = A\omega^S \tag{6}$$

where A represents a constant independent on temperature, ω related to angular frequency, ε_o demonstrates the dielectric permittivity in space (8.85×10^{-12} F/m), and s refer to the frequency exponent which commonly is minimal than or equal to one [28]. Figure 7 show the alteration of AC electrical conductivity with frequency in range of 100Hz to 5MHz It is observed that from the Figure 7, AC conductivity; σ_{ac} is increased with increase in frequency. Also; The AC conductivity is observed to be increased by ion irradiation and reach to maximum after irradiation by fluence $8x10^{16}$ion/cm^2. This indicates that there may be charge carriers which can be transported by hopping through the defect sites along the polymer chain. The frequency dependence of AC conductivity is the result of interface charge polarization.

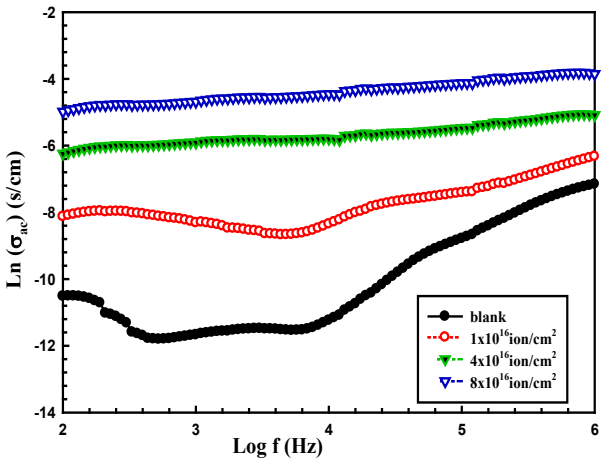

Fig. 7. Frequency and ion irradiation dependence of AC electrical conductivity.

Importantly, information about the dielectric and the conductivity relaxation behaviors of the pristine and irradiated films can be found from the complex electric modulus (M*), which is computed by the following expression [29]:

$$M^* = \frac{1}{\varepsilon^*} = M' + i\,M'' \tag{7}$$

Hence ε^* refers to the complex permittivity, M' and M'' are related to the real and imaginary part of the complex electric modulus, respectively. The electric modulus is used to reveal the conductivity relaxation by repressing the influence of electrode polarization. In which, M′ and M″ can be given from the impedance data using the following formulas [29]

$$\mathbf{M'} = \frac{\varepsilon'}{\varepsilon'^2+\varepsilon''^2} \tag{8}$$

$$\mathbf{M''} = \boldsymbol{\varepsilon''}/(\boldsymbol{\varepsilon'^2} + \boldsymbol{\varepsilon''^2}) \tag{9}$$

Figure 8 shows that the real part (M') of the electric modulus at low frequency close to zero value, which confirms that the polarization of electrode makes trivial contribution to the materials [30]. Moreover, M' values of the pristine and irradiated films increase with increasing the frequency and saturate at higher frequency region. It can also be noticed that M′ of the pristine film decreases after irradiation by ion beam owing to enhancing the polymer segmental movement, increasing the free carriers and conductivity [31]. Meanwhile, M′ gradually reduced with increasing the fluence of ion beam irradiation may be due to the increase in dipole mobility, therefore facility of the hopping mechanism [32].

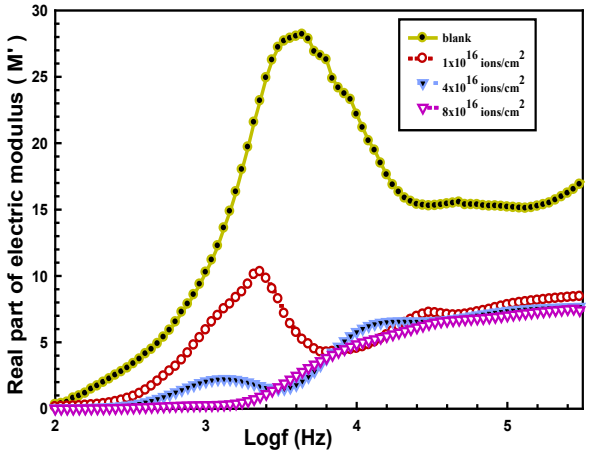

Fig. 8. Frequency dependence of real electric modulus for blank and irradiated PANI/Cu nanocomposite.

Meanwhile, the imaginary parts (M'') as a function of frequency of the blank and irradiated films are shown in Figure (9). One can be seen that values of M'' in the low-frequency region are very small, which suggests that motion of ions is occurred by hopping from position to adjoining position. The figure depicts the relaxation peaks, which represents the conductivity processes. In which, existence of relaxation peaks in M'' behaviors demonstrates that films are potential ionic conductors. Moreover, the intensity of relaxation peak of the pristine film is shifted to higher frequency after irradiation by ion beam, which supports that the time of relaxation τ_r reduced according to the following expression [33]:

$$\tau_r = \frac{1}{\omega_r} \tag{10}$$

where; ω_r is the angular frequency that ascribed to the crest of M″ versus log frequency curves. From the previous equation, we found that the relaxation time of the unirradiated **PANI/Cu** films is 8.9452×10^{-7} sec and decreases to 1.5186×10^{-7} sec, 4.6048×10^{-7} sec, and 4.3553×10^{-7} sec of the irradiated films by 1×10^{16}, 4×10^{16}, and 8×10^{16}, respectively. These reported results affirmed that the blank PANI/Cu nanocomposite films are improved after exposure to ion beam irradiation and become more convenient to high rapid optoelectronic devices.

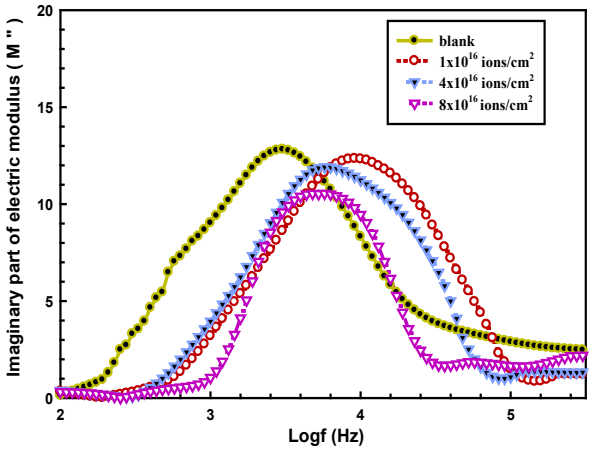

Fig. 9. Frequency dependence of imaginary electric modulus for blank and irradiated PANI/Cu nanocomposite.

For feasible application, the energy density (U) is computed based on the data of real part of the dielectric permittivity using the following formula [34]:

$$U = \frac{1}{2}\, \varepsilon' \varepsilon_O\, E^2 \tag{11}$$

where E represents the electric field that applied on the unirradiated and irradiated films and E = 1 V/mm. it can be observed a significantly increase in the energy density of PANI/Cu nanocomposite film after irradiation by different fluence of hydrogen ion beam as shown in Figure (10). Moreover, the energy density of the blank film is 1.5 $x10^{-5}$, which is increased to $2.1x10^{-5}$, $5x10^{-5}$ and $1.4x10^{-4}$ after irradiation by $1x10^{16}$ ions/cm^2 $4x10^{16}$, and $8x10^{16}$ions/cm^2 respectively. These results confirmed that the irradiation by ion beam improves the dielectric responses and properties of energy storage.

Table 1. ε', ε'', M', M'', σ_{ac}, and U of pure and treated PANI/Cu films at frequency 1000Hz.

samples	ε'	ε''	M'	M''	$U(J/m^3)$
PANI/Cu	1.5	16	10	9	0.000015
$1x10^{16}$ ions/cm^2	6	20	6	4	0.000021
4$x10^{16}$ ions/cm^2	10	58	3	3.6	0.00005
8$x10^{16}$ ions/cm^2	23	96	0.4	1.0	0.00014

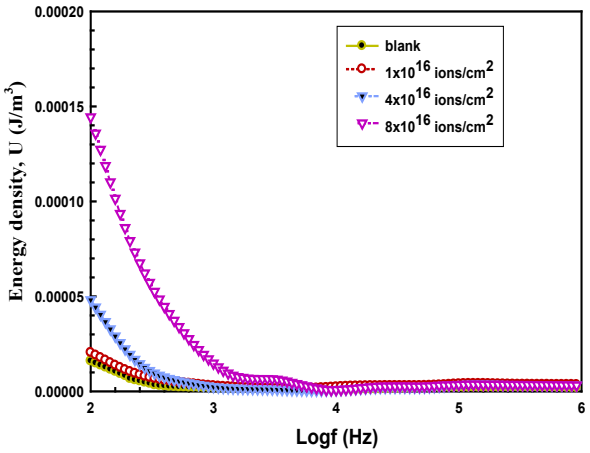

Fig. 10. Frequency and ion fluence dependences of the energy density.

4. Conclusion

The PANI/Cu nanocomposite film is prepared successfully using a homemade ion source sputtering technique. The XRD obtained that the crystallite size of film is 22nm and decreases after hydrogen ion irradiation to 20,18 and 14nm with fluence $1x10^{16}$, $4x10^{16}$ and $8x10^{16}$ ion.cm^{-2} respectively. The decrease in crystallite size of the irradiated film is due to the modifications of dislocation density. Electrical measurements confirm an improvement in the electrical conductivity and dielectric properties of the irradiated films. Also, the irradiated nanocomposite films have much dielectric than unirradiated film. Furthermore, a significant increases in the energy density efficiency of PANI/Cu film after exposure to ion beam. The reported improves in this study would open the way for utilizing irradiated nanocomposite films with a wide range of potential application, including batteries, supercapacitor, microelectronic devices

Acknowledgments

The authors extend their appreciation to the Deputyship for Research & Innovation, Ministry of Education in Saudi Arabia for funding this research work through the project number RI-44-0049

References

[1] Alotaibi BM, Al-Yousef HA, Alsaif NA and Atta A. (2022), Surface Innovations 40, 1-13; https://doi.org/10.1680/jsuin.22.00026

[2] Atta A, Abdelhamied MM, Abdelreheem AM and Berber MR (2021), Polymers 13(8): 1225; https://doi.org/10.3390/polym13081225

[3] Atta A, Abdelhamied MM, Abdelreheem AM and Althubiti NA (2022), Inorganic Chemistry Communications 135: 109085; https://doi.org/10.1016/j.inoche.2021.109085

[4] Abdeltwab E and Atta A (2021), Surface Innovations 40: 1-9.

[5] Althubiti NA, Atta A, Alotaibi BM and Abdelhamied MM (2022), Surface Innovations 40: 1-11; https://doi.org/10.1680/jsuin.22.00010

[6] Abdel-Galil A, Atta A and Balboul MR (2020), Surface Review and Letters 27(12): 2050019; https://doi.org/10.1142/S0218625X20500195

[7] Abdelhamied MM, Abdelreheem AM and Atta A (2021), Plastics, Rubber and Composites 51(1): 1-12; https://doi.org/10.1080/14658011.2021.1928998

[8] K.Chang; Tiny is Beautiful, Translating "Nano"into Practical, The New York Times (2005).

[9] A.M.Abdel Reheem, M.I.A.Abdel Maksoud and A.H.Ashour, Radiation Physics and Chemistry 125, 171-175 (2016); https://doi.org/10.1016/j.radphyschem.2016.04.010

[10] Atta A and Abdeltwab E (2022), Brazilian Journal of Physics 52(1): 1-10; https://doi.org/10.1007/s13538-021-01011-5

[11] A.M.Abdel Reheem, A.Atta, M.I.A.Abdel Maksoud, Radiation Physics and Chemistry 127, 269-275 (2016); https://doi.org/10.1016/j.radphyschem.2016.07.014

[12] Abdelhamied MM, Atta A, Abdelreheem AM, Farag ATM and El Sherbiny MA (2021), Inorganic Chemistry Communications 133: 108926; https://doi.org/10.1016/j.inoche.2021.108926

[13] Abdelhamid MM, Atta AA, Reheem AM, Ashour AH (2022), Surface Innovations 40:1-10; https://doi.org/10.1680/jsuin.22.01004

[14] Abdelhamied MM, Atta A, Abdelreheem AM, Farag ATM, and El Okr MM (2020), Journal of Materials Science: Materials in Electronics 31(24): 22629-22641; https://doi.org/10.1007/s10854-020-04774-w

[15] A. M. Abdel Reheem, A. Atta and T. Afify, Surface Review and Letters, 24, No. 3 (2017); https://doi.org/10.1142/S0218625X1750038X

[16] Atta A, Althubiti NA and Althubiti S (2021), Journal of the Korean Physical Society 79: 386-394; https://doi.org/10.1007/s40042-021-00224-w

[17] Abdel Reheem, A.M., et al., Review of Scientific Instruments, 2016. 87(8): p. 083302; https://doi.org/10.1063/1.4960394

[18] Ziegler, J.F., Biersack, J.P., 1982, SRIM Software, pp. 122-156; https://doi.org/10.1007/978-3-642-68779-2_5

[19] Popok, V.N. 2012, Rev. Adv. Mater. Sci. 30, 1-26.

[20] Abdeltwab E and Atta A (2021), International Journal of Modern Physics B 35(30): 2150310; https://doi.org/10.1142/S0217979221503100

[21] Reheem, A.A., M. Abdelhamid, and A. Ashour, Ion beam Effects on AC conductivity of Ge-Se-Bi films. Arab Journal of Nuclear Science and Applications, 2016.49(4): p. 31-40.

[22] Atta A, Abdelhamied MM, Essam D, Shaban M, Alshammari AH, Rabia M (2022), International Journal of Energy Research 46(5):6702; https://doi.org/10.1002/er.7608

[23] Atta A, Abdel Reheem AM and Abdeltwab E (2020), Surface Review and Letters 27(09): 1950214; https://doi.org/10.1142/S0218625X19502147

[24] Lotfy S, Atta A and Abdeltwab E (2018), Journal of Applied Polymer Science 135(15): 46146; https://doi.org/10.1002/app.46146

[25]Ahmed, H.T. and O.G. Abdullah, Polymers, 2019. 11(5): p. 853; https://doi.org/10.3390/polym11050853

[26] Vakil, P.N., et al., ACS omega, 2018. 3(10): p. 12813-12823; https://doi.org/10.1021/acsomega.8b01477

[27] Atta A (2020), Surface Innovations 9(1): 17-24; https://doi.org/10.1680/jsuin.20.00020

[28]Bouaamlat, H., et al., Dielectric Properties, Advances in Materials Science and Engineering, 2020; https://doi.org/10.1155/2020/8689150

[29] Abutalib M, Rajeh A., J Mater Sci: Mater Electron. 2020; 31, 9430-9442; https://doi.org/10.1007/s10854-020-03483-8

[30] Alghunaim NS., J Mater Res Technol. 2019;8(4):3596-3602; https://doi.org/10.1016/j.jmrt.2019.05.022

[31] Sunitha V, Radhakrishnan S., Polym Bull. 2020; 77(2), 655-670; https://doi.org/10.1007/s00289-019-02770-7

[32] Atta A, Lotfy S, Abdeltwab E., J Appl Polym Sci. 2018;135(33):46647; https://doi.org/10.1002/app.46647

[33] Fawzy YHA, Abdel-Hamid HM, El-Okr MM and Atta A (2018), Surface Review and Letters 25(03): 1850066; https://doi.org/10.1142/S0218625X1850066X

[34] Jilani, W., et al., Journal of Inorganic and Organometallic Polymers and Materials, 2019, 29(2), p. 456-464; https://doi.org/10.1007/s10904-018-1016-3